

## Coupled photocatalytic electron-transfers with 4,4'-bipyridinium derivatives of a betaine alkaloid from *Punica granatum*

Andreas Schmidt,<sup>\*a</sup> Thorsten Mordhorst,<sup>a</sup> Henning Fleischhauer,<sup>a</sup> and Gunnar Jeschke<sup>b</sup>

<sup>a</sup> Clausthal University of Technology, Institute of Organic Chemistry, Leibnizstrasse 6,  
D-38678 Clausthal-Zellerfeld, Germany

<sup>b</sup> Max Planck Institute for Polymer Research, Ackermannweg 10, D-55128 Mainz, Germany  
E-mail: [schmidt@ioc.tu-clausthal.de](mailto:schmidt@ioc.tu-clausthal.de)

Submitted in honor of the 75<sup>th</sup> birthday of Professor Alexandru Balaban

(received 08 Feb 05; accepted 22 Apr 05; published on the web 12 May 05)

---

### Abstract

Bis-hydroquinone substituted 4,4'-bipyridinium is the formal dimer of an alkaloid isolated from *Punica granatum* and can exist as dication, cross-conjugated as well as pseudo-cross-conjugated mesomeric betaine, and dianion. It can moreover form persistent radicals in the solid state as well as in solution due to redox reactions of the reducing and oxidizing partial structures. A reversible coupled photocatalytic process with proflavine as the sensitizer and EDTA as the sacrificial donor is presented. We performed ESR and ENDOR spectroscopy as well as DFT calculations to gain additional knowledge about the radical species.

**Keywords:** Radicals, ESR-spectroscopy, paraquat, mesomeric betaine, viologens

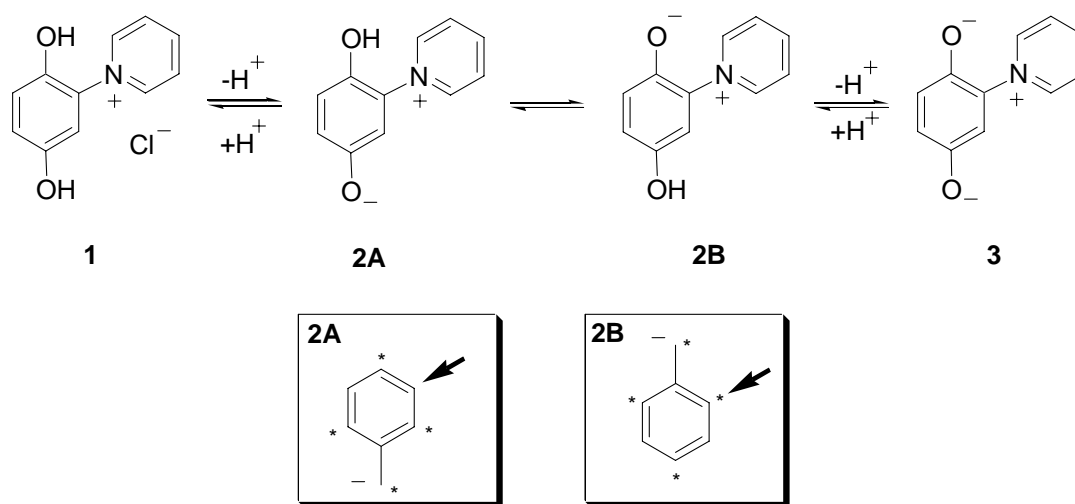
---

### Introduction

Natural products which belong to the class of heterocyclic mesomeric betaines form a relatively small class of compounds with interesting properties.<sup>1,2</sup> They are hybrids between naturally occurring organic cations (such as pyridinium alkaloids) and the very small group of anionic natural products.<sup>1</sup> In general, heterocyclic mesomeric betaines are divided into four major classes, *i.e.* conjugated (CMB), cross-conjugated (CCMB), pseudo-cross-conjugated heterocyclic mesomeric betaines (PCCMB), and *N*-ylides which form a subclass of CMB.<sup>3</sup> We recently focussed our interest on an alkaloid betaine which was isolated from the leaves of *Punica granatum*,<sup>4</sup> and synthesized some derivatives.<sup>5</sup> Although this *Punica* alkaloid **2** possesses a very simple structure which is related to the redox systems of the respiratory chain (ubiquinone / NAD<sup>+</sup>) as well as photosynthesis (plastoquinones), it is a highly unusual alkaloid for a couple of reasons. First, only two pyridinium-phenolates have been isolated to date from natural sources,<sup>1</sup>

although the pyridinium ring is present in all four major classes of heterocyclic mesomeric betaines. Second, we found that this alkaloid can exist as a cation **1**, in which form it seemingly was isolated,<sup>4</sup> as two distinct types of heterocyclic mesomeric betaine **2A/B**, or as an anionic species **3**.<sup>6</sup> The tautomer **2A** is a cross-conjugated mesomeric betaine; the cationic partial structure is joined to the negative structure element through an unstarred position of the isoconjugated equivalent, the benzyl anion (Scheme 1). This architecture causes a delocalization of the charges in separated parts of the common  $\pi$ -electron system. In the tautomer **2B**, which represents a conjugated mesomeric betaine, the cationic partial structure is joined through a starred position of the isoconjugated benzyl anion. As a consequence, common atoms for either charge exist in the canonical formulae. Betaines, which belong to two distinct classes are very rare.<sup>7</sup>

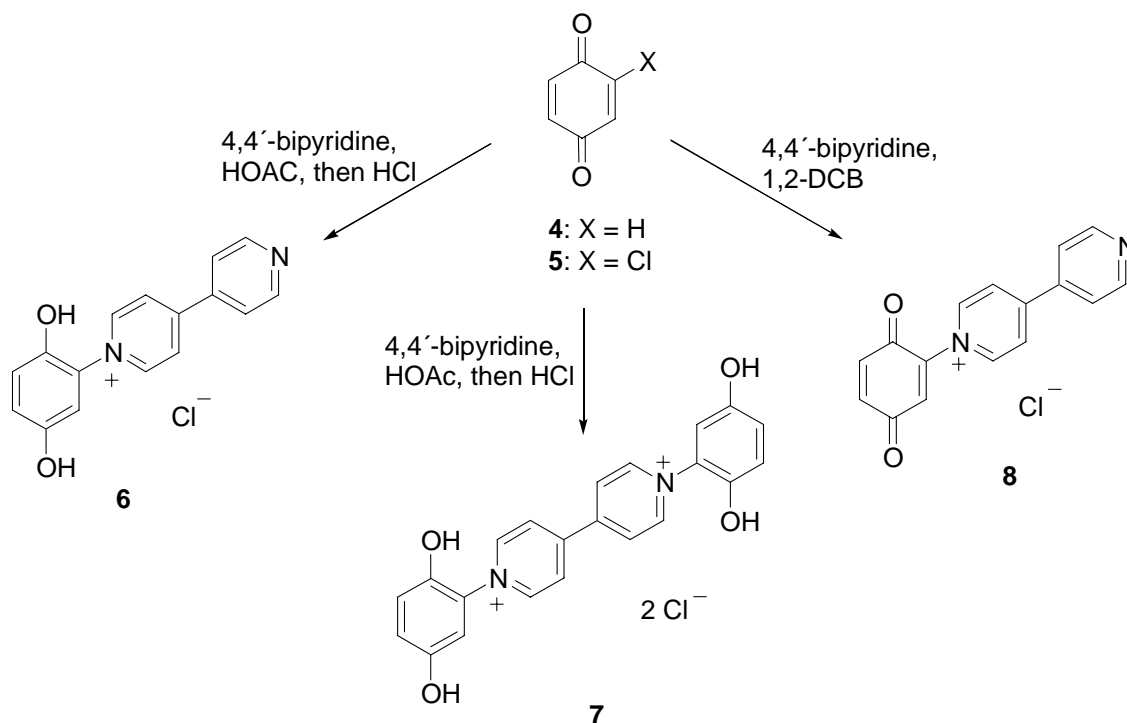
We wish to report here the results concerning the synthesis and properties of the 4,4'-bipyridinium derivative of alkaloid **1**. We were stimulated by the fact that photocatalytic reductions of methylviologen ( $MV^{2+}$ ) in the presence of several sensitizers,<sup>8</sup> or the photochemical decomposition of water to hydrogen<sup>9</sup> *via* the  $MV^{+\bullet}$  radical still remain interesting topics of current research. Less attention, however, has been focussed on derivatives of the substitution pattern of the 4,4'-bipyridinium itself.<sup>10</sup> Recent examples are the combination of methyl viologen with iron porphyrins,<sup>11</sup> and the synthesis of viologens with extended  $\pi$ -conjugation.<sup>12</sup> The  $MV^{+\bullet}$  radical can be recognized by enzymes such as hydrogenase,<sup>13</sup> formate dehydrogenase,<sup>14</sup> nitrate as well as nitrite reductase,<sup>15</sup> and glutathione reductase.<sup>16</sup> Host-guest properties were also reported<sup>17</sup> and the isolation and X-ray analysis of the  $PF_6^-$  salt was presented.<sup>18</sup> The 4,4'-bipyridinium derivative of the *Punica* alkaloid **2** combines typical donor (benzene-1,4-diol) and acceptor (viologen) structure elements which have individually attracted considerable attention due to their ability to form CT complexes with interesting photo and electronic properties.<sup>19</sup>



Scheme 1

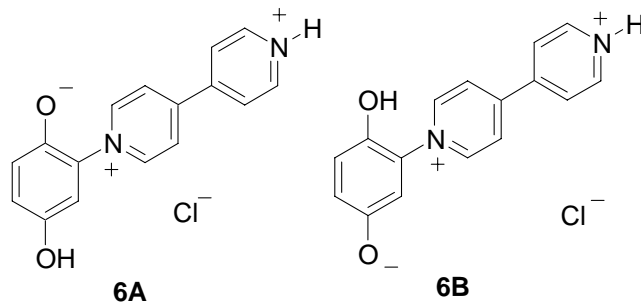
## Results and Discussion

The synthesis of a 4,4'-bipyridinium derivative of the *Punica* alkaloid starts from *p*-benzoquinone **4** and 4,4'-bipyridine (Scheme 2). Conducting the reaction in acetic acid, followed by the addition of excess hydrochloric acid to exchange the anion to chloride, results in the formation of the hydroquinone **6** which is orange-brown in color; more vigorous conditions lead to the formation of the symmetric bipyridinium compound **7** as dark crystals which include one molecule of water of crystallization per molecule of **7**. Starting from chlorobenzoquinone **5**, the reaction conducted in 1,2-dichlorobenzene as solvent yields the quinone **8** which proved to be very sensitive toward traces of water, so that it could not be characterized completely. In electrospray mass spectrometry, a prominent peak at  $m/z$  263 u clearly indicates the existence of the molecule in a mixture with hydroquinone **6**.



**Scheme 2**

Indicative for the formation of tripolar tautomers such as **6A** and **6B** (Scheme 3), the OH-groups of **6** are not detectable in DMSO- $d_6$  by  $^1\text{H}$  NMR spectroscopy, and the signals of the  $\alpha$ - and  $\beta$ -hydrogens of the pyridinium ring are slightly shifted downfield in comparison to non-protonated pyridine substituents.<sup>5</sup>



### Scheme 3

Two  $pK_a$  values of 7, 6.9 and 10.3, were determined by titration of 100 mL of a 0.01 M solution of **7** in water with 0.1 M HCl and 0.1 M NaOH, respectively. These results resemble the *Punica* alkaloid **1**, which has two  $pK_a$  values at 6.9 and 10.2. Obviously, the acidities of the hydroquinone moieties of one part of the molecule are not influenced by the second hydroquinone. The titration curve of **7** is presented in Figure 1. A concentrated solution of **7** in water has  $pH$  3.6, so that a mesomeric betaine such as **9** is formed in solution which (similar to alkaloid **2**<sup>5,6</sup>) cannot be distinguished spectroscopically from its tautomers and which is presented in Scheme 4. The salt **7** and the betaine **9** have absorption maxima  $\lambda_{max} = 286.0$  nm, measured in HCl at  $pH$  1.4 and  $pH$  6.8. The betaine displays an additional strong shoulder at  $\lambda_{max} = 260$  nm (Figure 2). It is intensely orange in color and slowly decomposes as a solid in air such that it could only be characterized in solution. As expected, all  $^1H$  NMR signals are considerably shifted upfield on neutralisation of **7**.

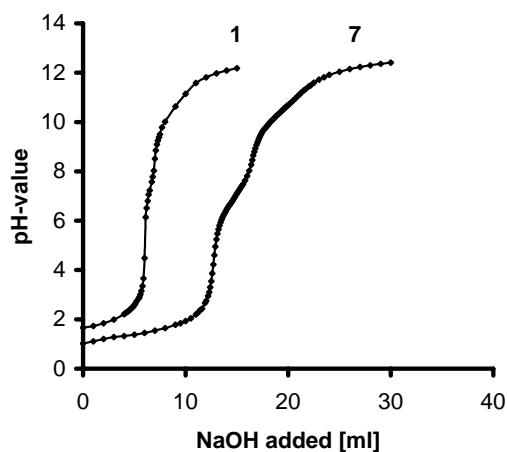


**Figure 1.** Titration curves of 100 ml 0.01 M solution of *Punica* alkaloid **1** and **7**, respectively, with 0.1 M NaOH.

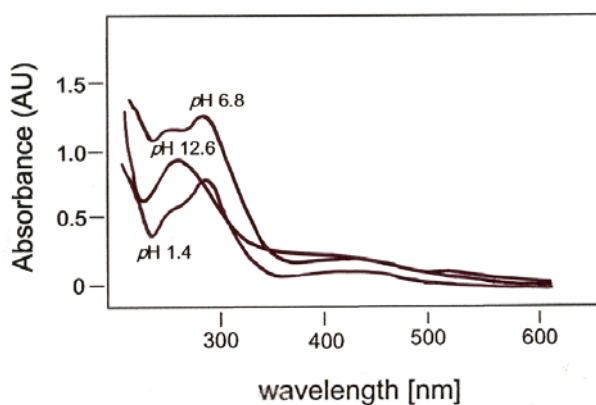
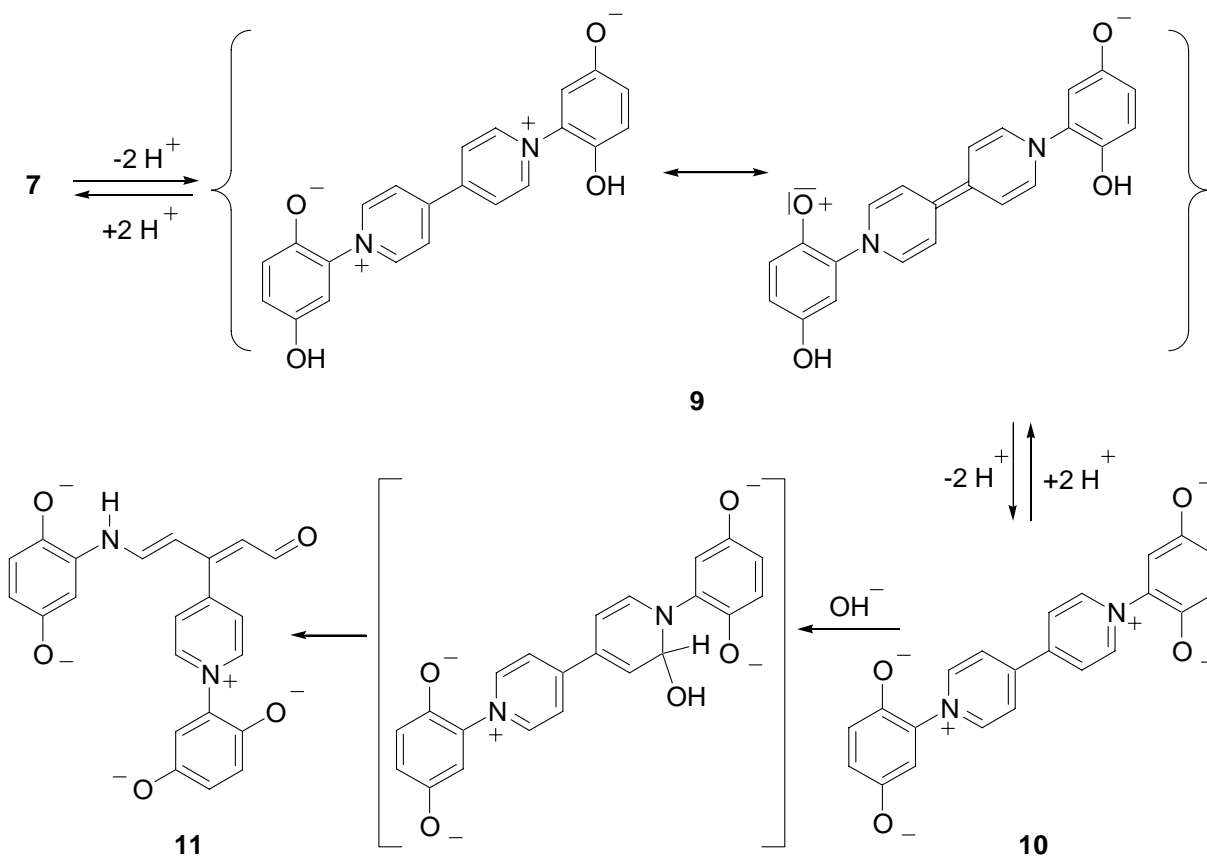


**Figure 2.** Qualitative UV spectra at different  $pH$  values (0.11 mmol/100 mL of water).

The  $pK_a$ -value at 10.3 indicates the formation of a dianionic species **10**, which is formed as an orange, unstable compound in air. At  $pH$  12.6, adjusted by the addition of NaOH to the aqueous solution of **7**, this species gives an absorbance at  $\lambda_{max} = 260.0$  nm (Figure 2). On gentle warming, decomposition with loss of one molecule of benzene-1,2,4-triolate occurs as evidenced by  $^1H$  NMR spectroscopy. A pericyclic ring cleavage to pentadienals such as **11** was not detected until the solution was heated at  $pH$  12. Then, the crude NMR spectra provide evidence for the formation of non-isolable ring-cleaved products similar to *Fujiwara* compounds<sup>20</sup> in addition to considerable amounts of as yet unidentified by-products (Scheme 4).

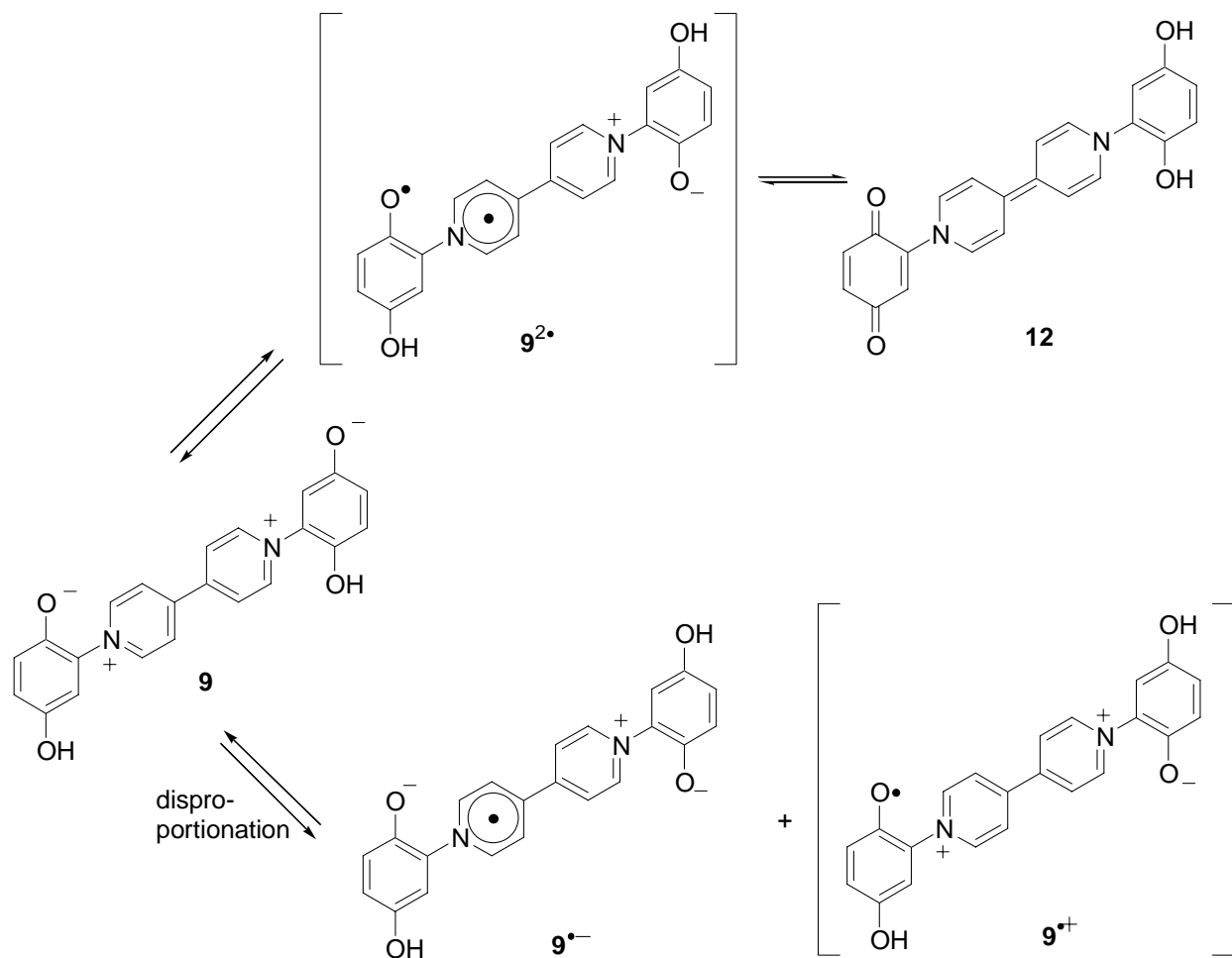


**Scheme 4**

In contrast to the *Punica* alkaloid **2**, the 4,4'-bipyridinium derivative **9** can be classified as a hybrid between a cross-conjugated (CCMB) and a pseudo-cross-conjugated mesomeric betaine (PCCMB) according to the classification by *Ollis, Stanforth* and *Ramsden*.<sup>3</sup> Thus, deprotonation of the 5'-OH group results in the formation of a CCMB with positive and negative charges which are restricted to separate parts of the molecule, whereas deprotonation of the 2'-OH group yields a PCCMB. Electron sextet structures without internal octet stabilization, which can be drawn as one of several canonical formulae, are characteristic for pseudo-cross-conjugation (Scheme 4).<sup>1,2,3</sup> Although these electron-sextet formulae have only a small contribution, if at all, to the

overall-electronic structure of the molecule, the charges are effectively, but obviously not exclusively, delocalised in separated parts of the common  $\pi$ -electron system.<sup>3</sup> Accordingly, common sites for positive and negative charges exist in the canonical formulae.

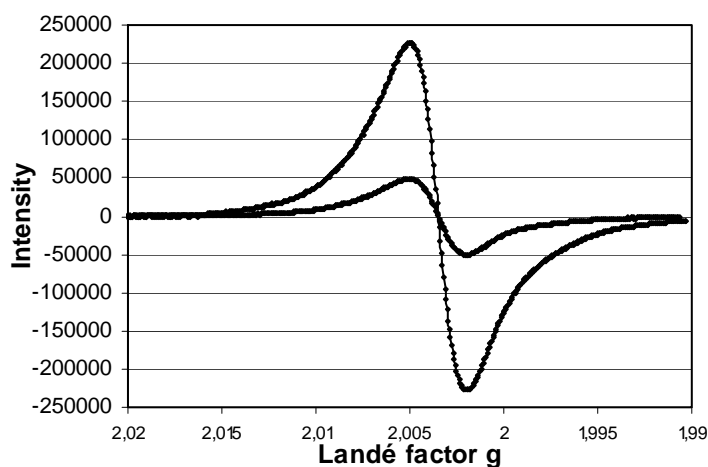
Under an inert atmosphere, however, addition of base to a solution of **7** results in a sudden change of the color to intense blue, which - at least in part - is due to the formation of radical species. This color disappears on acidification, on addition of  $K_3[Fe(CN)_6]$ , and on addition of sodium dithionite. Basification under these conditions results in an upfield shift of the resonance frequencies, which broaden considerably as the blue color develops. *A priori*, two distinct types of redox reaction can be taken into consideration. An intramolecular electron transfer from the reducing deprotonated hydroquinone moiety (1,4-benzenediolate) to the 4,4'-bipyridinium ring would lead to diradical species such as **9**<sup>2•</sup> (Scheme 5) which could then result in the formation of quinoidal structures such as **12** after tautomerisation.



Scheme 5

However, no trace of this compound **12** was ever observed spectroscopically. On the other hand, a disproportionation of two molecules of **9** would lead to radical anions  $\mathbf{9}^{\bullet-}$  and radical cations  $\mathbf{9}^{\bullet+}$ . The former mentioned radical anions resemble known persistent radicals formed from methyl viologen and are known to be persistent and blue in color.<sup>10,22</sup>

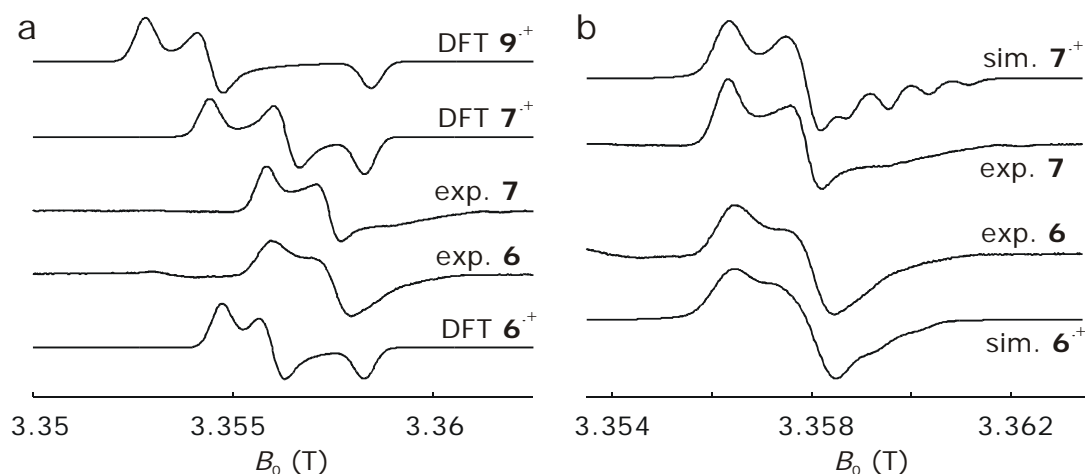
In order to gain additional knowledge about the radicals and to study protonated as well as non-protonated species, we performed some ESR studies on the salts **6** and **7** as solids, and on the mesomeric betaine **9** in solution. The ESR spectra of **7** in the solid state and in triethylamine solution, in which the mesomeric betaine **9** is formed, are shown in Figure 3. The ESR spectra consist of broad singlets centered at  $g = 2.00349$  without observable hyperfine splittings. It is evident, that addition of base causes a considerable intensification of the ESR signal indicating that more free radicals are generated under these conditions.



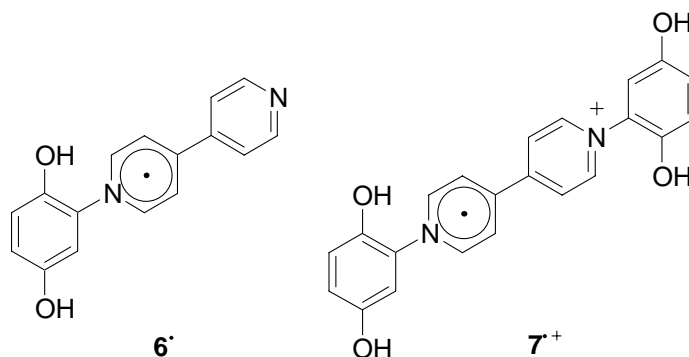
**Figure 3.** ESR spectra of solid **7** and as a concentrated solution in  $\text{NEt}_3$ .

Figure 4 shows the ESR spectra of the solid compounds **6** and **7** at approximately 9.8 GHz and 94 GHz, as well as the theoretical spectra of radicals  $\mathbf{6}^{\bullet}$ ,  $\mathbf{7}^{\bullet+}$  (Scheme 6) and  $\mathbf{9}^{\bullet-}$  simulated for  $g$  tensors calculated by the DFT method using the BLYP functional, and disregarding any hyperfine couplings.

A DFT computation was also performed for radical  $\mathbf{9}^{\bullet+}$ . The corresponding spectrum is not shown as it extends to much lower fields (3.345 T) than the experimental spectra ( $g_x = 2.0098$ ). Furthermore, the smallest principal component of the computed  $g$  tensor of radical  $\mathbf{9}^{\bullet+}$  of 2.0026 is larger than the free electron  $g$  value of  $g_e = 2.0023$ , while the experimentally observed and all other computed  $g$  tensors have one principal component  $g_z$  that is smaller than  $g_e$ . We may thus safely rule out that the observed radical is formed by a one-electron reduction. It is also apparent that the computed spectrum of radical  $\mathbf{7}^{\bullet+}$  is a better fit to the experimental spectrum than the computed spectrum for the betaine form  $\mathbf{9}^{\bullet-}$ .



**Figure 4.** High-field ESR spectra taken at approx. 94 GHz and simulated spectra corresponding to  $g$  tensors computed by DFT. a) Overview with simulations that disregard hyperfine couplings. (b) Simulation for radical  $7^{\cdot+}$  assuming idealized relative orientations of  $g$  and hyperfine tensors and parameters that provide the best fit of the experimental spectrum of  $7$  within this simplified model.



### Scheme 6

Closer inspection of the experimental spectra reveals that their high-field edges corresponding to the  $g_x$  component are substantially broadened. This is unlikely to be due to  $g$  strain, as the deviation from  $g_e$  is relatively small. The broadening must thus be attributed to hyperfine couplings, which are not included in the simulation. Indeed, a DFT computation of the hyperfine couplings of radical  $7^{\cdot+}$  reveals that the  $^{14}\text{N}$  hyperfine tensors are nearly axial with the unique principal component of approximately 22 MHz, which is the largest component, roughly along the  $g_x$  axis. The computed angles between the unique axis of the hyperfine tensors and the  $g_x$  axis are  $6^\circ$  and  $15^\circ$  for the two nitrogen nuclei. A similar situation is found for radical  $6^{\cdot}$ . However, in this case the computed unique principal components of the  $^{14}\text{N}$  hyperfine tensors are 23 MHz for the substituted nitrogen atom and only 13 MHz for the unsubstituted one. According to the same DFT computations, hyperfine broadening at the  $g_y$  and  $g_z$  components is mainly due



to the aromatic protons next to the substituted nitrogens. For radical **6** $\cdot$ , there are two such protons with maximum hyperfine couplings of 18 MHz, while for radical **7** $\cdot^+$  there are four such protons with maximum hyperfine couplings of 7.5 MHz. This finding is in line with the stronger broadening at the the  $g_y$  and  $g_z$  components for radical **6** $\cdot$ , which are caused by the larger maximum coupling.

Based on these findings, we tried to fit the high-field ESR spectra by simplified parameter sets with coincident principal axes frames for the hyperfine and  $g$  tensors and by explicitly considering only hyperfine couplings to the nitrogen nuclei and the adjacent aromatic protons (Figure 4b). All remaining hyperfine couplings were simulated by a global Gaussian line broadening parameter of 13 MHz for radical **6** $\cdot$  and 8 MHz for radical **7** $\cdot^+$ . We found that we had to change the  $g$  values compared to the DFT results to obtain satisfying agreement. Furthermore, all proton hyperfine couplings had to be scaled by 50%, while the values for the nitrogen couplings could be retained. Except for the resolution of the  $^{14}\text{N}$  hyperfine coupling along  $g_z$  that is not observed in the experiments, the simulated spectra agree quite well with the experimental ones. The inferior resolution of the experimental spectra in this region may be partially due to the non-coincidence of the principal frames, but may also indicate some variation in the parameters due to crystal strain. In the ENDOR spectrum of **7** at approximately 9.8 GHz,  $^{14}\text{N}$  couplings  $A(^{14}\text{N}) = 4.5$  MHz are observable together with poorly resolved and relatively uncharacteristic hyperfine splittings to the protons (Figure 5). The  $^{14}\text{N}$  couplings are in the expected range for the singularity of the hyperfine powder pattern for both radicals **7** $\cdot^+$  and **9** $\cdot^-$ .

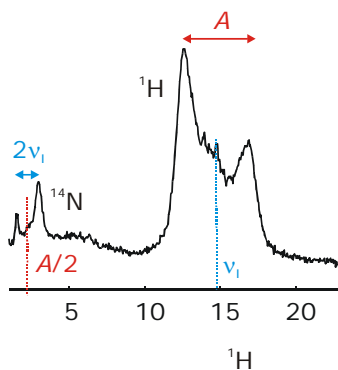
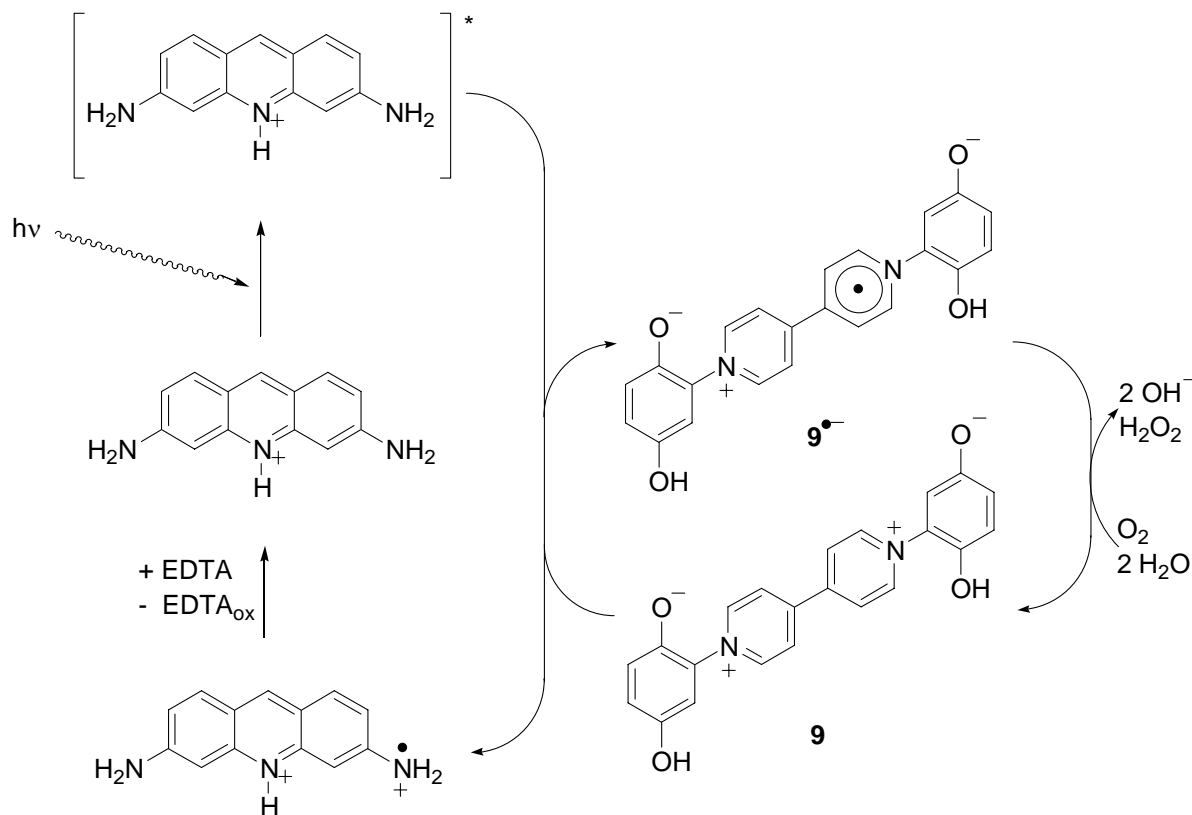


**Figure 5.** Solid-state ENDOR spectrum of **7** at approximately 9.8 GHz (80 K).

The radical anion **9** can be generated in solution in coupled photocatalytic processes involving energy- and electron-transfers with proflavine as sensitizer (Scheme 7). Thus, irradiation of a neutral aqueous solution of catalytic amounts of acridinium-3,6-diamine (proflavinium;  $pK_a = 9.65$  in water<sup>21</sup>), excess ethylenediamine-tetraacetic acid disodium salt (EDTA), and the mesomeric betaine **9** results in the formation of a dark greenish-blue mixture within a couple of minutes in an inert atmosphere. In contrast to photoreductions of methylviologen<sup>22</sup> the process obviously begins with the reduction of the mesomeric betaine **9** to the corresponding monoanion radical **9** by the proflavinium in its excited state, generated by light

absorption at  $\lambda_{\text{max}} = 445$  nm. The resulting oxidized photocatalyst is regenerated by reductive quenching with the two-electron donating agent EDTA<sup>23</sup> which is the sacrificial donor of this cycle. On exposure to air the mesomeric betaine **9** is regenerated quantitatively by reoxidation of **9**<sup>•-</sup>, observable by a spontaneous change of the color of the solution from dark greenish-blue to pale yellow. This cycle can be repeated numerous times, as no decomposition products of the starting material proflavine and **9** are detectable even after prolonged irradiation times. Under an inert atmosphere, the radical is persistent for several hours at room temperature.



### Scheme 7

In UV spectroscopy under nitrogen the radical anion **9**<sup>•-</sup> can be identified by a broad absorption maximum at  $\lambda_{\text{max}} = 380$  nm and a small shoulder at approximately 590 nm. As the radical forms, the peak of the starting material at  $\lambda_{\text{max}} = 286$  nm disappears.

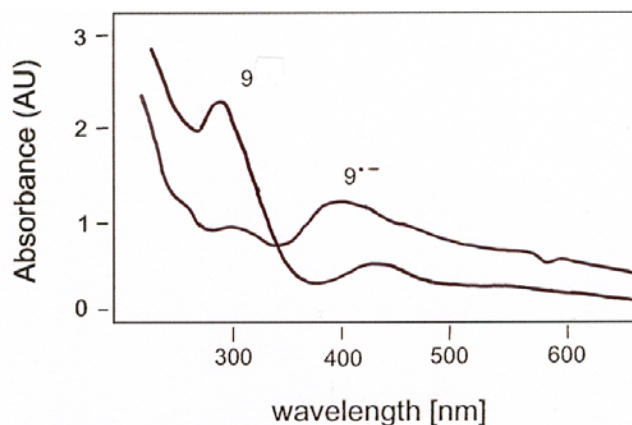


**Figure 6.** UV-spectra of betaine **9** and its radical in water.

The reaction of the related methyl viologen radical cation MV with oxygen is quantitative and can be used to detect very low concentrations of oxygen.<sup>24</sup> It is reduced in two steps from O<sub>2</sub> to O<sub>2</sub> (or HO<sub>2</sub>) and then to HO<sub>2</sub><sup>-</sup> (or H<sub>2</sub>O<sub>2</sub>),<sup>25</sup> whereas the reduction of H<sub>2</sub>O<sub>2</sub> was found to be a slow process.<sup>26</sup> O<sub>2</sub> and H<sub>2</sub>O<sub>2</sub> have been considered to be responsible for the herbicidal activity of methyl viologen.<sup>27</sup> The reversible photocatalytic process of **9** under the conditions described here can therefore be monitored by determining the pH of the reaction medium with time (Figure 7).

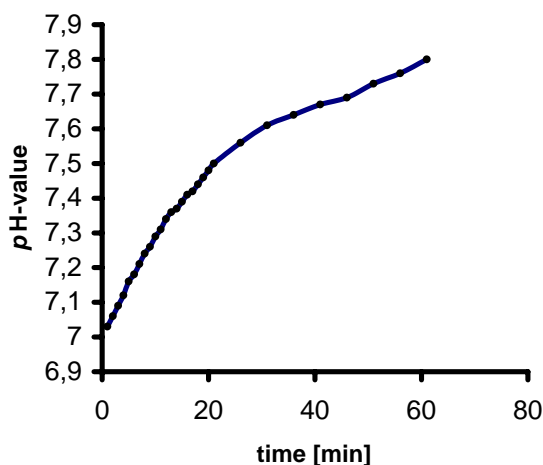


**Figure 7.** Changing of the pH value with time on irradiation and subsequent exposure to oxygen.

In summary, we present a simple derivative of a natural product, which possesses interesting properties as a heterocyclic mesomeric betaine and as a radical species.

## Experimental Section

**General Procedures.** The  $^1\text{H}$  and  $^{13}\text{C}$  NMR spectra were recorded on Bruker ARX-400 and DPX-200 spectrometers. Multiplicities are described by using the following abbreviations: s = singlet, d = doublet, m = multiplet. FT-IR spectra were obtained on a Bruker Vektor 22 in the range of 400 to 4000  $\text{cm}^{-1}$  (2.5 % pellets in KBr). The ESI mass spectra were measured with an Agilent LCMSD Series HP1100 with APIES. Samples were sprayed from methanol at 0 V fragmentor voltage unless otherwise noted. The solid-state EPR and Davies ENDOR spectra were recorded on Bruker E580 (9.8 GHz) and E680 (95 GHz) spectrometers and the solvent-dependent ESR spectra were recorded on a Bruker ER-200D SRC (9.4 GHz). Density functional theory (DFT) calculations were performed with the ADF2002.1 package,<sup>28</sup> using the BLYP functional. The structures were optimized by spin-restricted computations using the TZP basis set with an effective core potential for the inner shell for carbon, nitrogen, and oxygen and no symmetry constraints. Hyperfine couplings (spin-unrestricted) and  $g$  tensors were computed with TZ2P all-electron basis sets. For  $g$  tensors, a spin orbit-relativistic spin-restricted computation was performed within the zero-order regular approximation (ZORA) formalism.<sup>29</sup> Solid-state ESR spectra were simulated with the WIN-EPR Simfonia program from Bruker.

***N*-(2''-5''-Dihydroxyphenyl)-4-(4'-pyridine)pyridinium chloride (6).** A sample of 4.32 g (40 mmol) of *p*-benzoquinone was suspended in 20 mL of glacial acetic acid and treated with 6.25 g (40 mmol) of 4,4'-bipyridine. The resulting mixture was diluted with 10 mL of water, and heated, whereupon 12 mL of 18% hydrochloric acid were added. After cooling, the mixture was treated with 300 mL of ether and warmed at reflux. The resulting brown solid was collected by filtration, washed with water, and dried *in vacuo*. Recrystallization from water yielded 6.4 g of a pale brown solid (51%), mp. 128°C. IR:  $\nu_{\text{max}}$  (KBr)/ $\text{cm}^{-1}$ : 3423, 2580, 1632, 1511, 1209, 818. UV (MeOH):  $\lambda_{\text{max}}$  295, 392 nm.  $^1\text{H}$  NMR (DMSO- $d_6$ ):  $\delta$  = 9.27 (2H, d,  $^3J$  = 7.0 Hz), 8.90 (2H, dd,  $^3J$  = 4.6 Hz,  $^5J$  = 1.5 Hz), 8.69 (2H, d,  $^3J$  = 7.0 Hz), 8.10 (2H, dd,  $^3J$  = 4.6 Hz,  $^5J$  = 1.5 Hz), 7.12 (1H, d,  $^3J$  = 2.6 Hz), 7.70 (1H, s), 7.00 (1H,  $^3J$  = 2.6 Hz) ppm.  $^{13}\text{C}$  NMR (DMSO- $d_6$ ):  $\delta$  = 149.4 (2C), 147.8 (2C), 146.4, 144.9, 142.1 (2C), 125.8 (2C), 124.7 (2C), 117.6 (4C) ppm. ESIMS:  $m/z$  = 263 ( $\text{M}^+$ , 20), 156.2 (100). Anal. Calcd. for  $\text{C}_{16}\text{H}_{15}\text{ClN}_2\text{O}_3$  (1 mol of water of crystallization): C, 60.29; H, 4.74; N, 8.79. Found: C, 61.50; H, 4.66; N, 8.77.

***N,N'*-Bis-(2'',5''-dihydroxyphenyl)-4,4'-dipyridinium dichloride (7).** A sample of 2.70 g (25 mmol) of *p*-benzoquinone was suspended in 50 mL of glacial acetic acid and treated with 1.95 g (12.5 mmol) of 4,4'-bipyridine. After heating at reflux temperature over a period of 3 h, the mixture was treated with excess concentrated hydrochloric acid. After cooling, 300 mL of ether were added whereupon crystals separated which were filtered off, washed with cold water and dried *in vacuo*. After recrystallization from water 4.65 g of dark violet crystals were obtained in quantitative yield, mp. 255 °C. IR:  $\nu_{\text{max}}$  (KBr)/ $\text{cm}^{-1}$ : 3027, 2360, 1624, 1511, 1208, 839, 792. UV (MeOH):  $\lambda_{\text{max}}$  290, 450 nm.  $^1\text{H}$  NMR (DMSO- $d_6$ ):  $\delta$  = 10.52 (2H, s), 9.74 (2H, s), 9.53 (4H, d,  $^3J$  = 7.0 Hz), 8.96 (4H, d,  $^3J$  = 7.0 Hz), and 7.10 (6H, m) ppm.  $^{13}\text{C}$  NMR (DMSO- $d_6$ ):  $\delta$  =

149.5 (2C), 147.3, 141.8 (2C), 130.4 (2C), and 116.2 (4C) ppm. ESIMS:  $m/z = 373$  ( $M^+$ , 100), 187 ( $M^{2+}$ , 33). Anal. Calcd. for  $C_{22}H_{20}Cl_2N_2O_5$  (1 mol of water of crystallization): C, 57.03; H, 4.35; Cl, 15.30; N, 6.05; O, 17.27. Found: C, 57.03; H, 4.17; Cl, 14.98; N, 5.49; O, 18.33.

**4,4'-Dipyridinium-*N,N'*-bis-(5''-hydroxyphenyl-2''-diolate) / 4,4'-Dipyridinium-*N,N'*-bis-(2''-hydroxyphenyl-5''-diolate) (9).** A column was filled with 60 mL of Amberlite IRA-402 which was washed with 800 mL of distilled water. Then, the resin was treated with 80 mL of a 4 % sodium hydroxide solution. After 15 minutes, the anion exchange resin was washed with water until the eluant had  $pH$  7, and then with 100 mL of a water/ethanol mixture (3:1). The pyridinium salt **7** (200 mg; 0.45 mmol) was dissolved in the same solvent mixture, added to the resin and eluted immediately. The eluant was evaporated to dryness, and the dark residue was dissolved in ethanol. This compound is not stable in the solid state.  $^1H$  NMR ( $D_2O$ ):  $\delta = 8.91$  (4H; d,  $^3J = 5$  Hz), 8.45 (4H, d,  $^3J = 5$  Hz), 6.52 (6H, m) ppm.  $^{13}C$  NMR ( $D_2O$ ):  $\delta = 155.1$  (2C), 149.1 (4C), 146.7 (4C), 132.5 (2C), 126.3 (4C), 124.4 (2C), 122.4 (2C), 113.3 (2C) ppm.

**Coupled photocatalytic electron-transfer.** Ethylenediamine-tetraacetic acid disodium salt (0.14 g) was dissolved in 5 mL of water and was mixed with a solution 3.21 mg of 3,6-diaminoacridine hemisulfate in 10 mL of water. Then, a 10 mL aqueous solution of 15 mg of the betaine **9** and 285 mL of water were added. This mixture was placed in the reactor. Nitrogen was then bubbled through the solution for 15 min before the medium-pressure 150W mercury lamp was switched on. After a couple of minutes, an intense blue-greenish color develops which disappears immediately on bubbling air through the solution. After a 10-minutes washing time with nitrogen, this cycle can be started again. Irradiation while the mixture is exposed to air results in an increasing  $pH$  of the solution.

## Acknowledgements

Dr. Heinz Vollmer, Clausthal University of Technology, Institute of Physics and Physical Technologies, is gratefully acknowledged for measuring the solvent-dependent ESR spectra.

## References

1. Schmidt, A. *Adv. Heterocyclic Chem.* **2003**, *85*, 67.
2. Schmidt, A. *Curr. Org. Chem.* **2004**, *8*, 653.
3. Ollis, W. D.; Stanforth, S. P.; Ramsden, C. A. *Tetrahedron* **1985**, *41*, 2239.
4. Nawwar, M. A. M.; Hussein, S. A. M.; Merfort, I. *Phytochemistry* **1994**, *37*, 1175.
5. Schmidt, A.; Mordhorst, T. *ARKIVOC* **2003**, (*xiv*), 233.
6. Schmidt, A.; Mordhorst, T.; Nieger, M. *Nat. Prod. Res.* **2005**, in press.
7. Schmidt, A.; Kindermann, M. K.; Nieger, M. *Heterocycles* **1999**, *51*, 237.

8. (a) Islam, S. D.-M.; Konishi, T.; Fujitsuka, M.; Ito, O.; Nakamura, Y.; Usui, Y. *Photochem. Photobiol.* **2000**, *71*, 675. (b) Tsukahara, K.; Sawai, N.; Hamada, S.; Nakazawa, T.; Nakagaki, R. *Bull. Chem. Soc.* **1995**, *68*, 1947. (c) Kalyanasundaram, K.; Gräzle, M. *Helv. Chim. Acta* **1980**, *63*, 478. (d) Okura, I.; Thuan, N. K. *J. Chem. Soc., Faraday Trans.* **1980**, *78*, 2209. (e) Krüger, W.; Fuhrhop, J.-H. *Angew. Chem.* **1982**, *94*, 132.
9. de Jongh, P. E.; Vanmaekelbergh, D.; Kelly, J. J. *Chem. Comm.* **1999**, 1069.
10. Monk, P. M. S. *The Viologens, Physicochemical Properties, Synthesis and Applications of the Salts of 4,4'-Bipyridine*; John Wiley & Sons: Chichester, 1998.
11. (a) Koga, H.; Hamada, T.; Sakaki, S. *J. Chem. Soc., Dalton Trans.* **2003**, 1153. (b) Sakaki, S.; Koga, H.; Tao, K.; Yamashita, T.; Iwashita, T.; Hamada, T. *J. Chem. Soc., Dalton Trans.* **2000**, 1015.
12. Nanasawa, M.; Miwa, M.; Hirai, M.; Kuwabara, T. *J. Org. Chem.* **2000**, *65*, 593.
13. (a) Kinumi, Y.; Okura, I. *J. Mol. Catal.* **1989**, *52*, L33. (b) Katz, E.; Kozlov, Y. N.; Kiselev, B. A. *Biofizika* **1979**, *24*, 801.
14. Mandler, D.; Willner, I. *J. Chem. Soc., Perkin Trans 2* **1988**, 997.
15. Willner, I.; Lapidot, N.; Riklin, A. *J. Am. Chem. Soc.* **1989**, *111*, 1883.
16. Willner, I.; Lapidot, N.; Riklin, A.; Kasher, R.; Zahavy, E.; Katz, E. *J. Am. Chem. Soc.* **1994**, *116*, 1428.
17. (a) Jeon, W. S.; Kim, H.-J.; Lee, C.; Kim, K. *Chem. Comm.* **2002**, 1828. (b) Yoshikawa, H.; Nishikiori, S. *Chem. Lett.* **2000**, 142. (c) Yoshikawa, H.; Nishikiori, S.; Suwinska, K.; Luboradzki, R.; Lipkowski, J. *Chem. Commun.* **2001**, 1398. (d) Yoshikawa, H.; Nishikiori, S.; Watanabe, T.; Ishida, T.; Watanabe, G.; Murakami, M.; Suwinska, K.; Luboradzki, R.; Lipkowski, J. *J. Chem. Soc., Dalton Trans.* **2002**, 1907.
18. Bockman, T. M.; Kochi, J. K. *J. Org. Chem.* **1990**, *55*, 4127.
19. (a) Kidowaki, M.; Tamaoki, N. *Chem. Comm.* **2003**, 290. (b) Kim, H.-J.; Heo, J.; Jeon, W. S.; Lee, E.; Kim, J.; Sakamoto, S.; Yamaguchi, K.; Kim, K. *Angew. Chem.* **2001**, *113*, 1574.
20. Schmidt, A.; Nieger, M. *J. Chem. Soc., Perkin Trans 1* **1999**, 1325.
21. Albert, A. *The Acridines*, 1<sup>st</sup> Ed.; London, 1951, p 114.
22. (a) Tausch, M. W. *PdN-Chemie* **1994**, *43(3)*, 13. (b) Korn, S.; Tausch, M. W. *PdN-Chis* **2000**, *49*, 29; Korn, S.; Tausch, M. W. *J. Chem. Educ.* **2001**, *78*, 1238. (c) Wöhrle, D.; Tausch, M. W.; Stohrer, W.-D. *Photochemie - Konzepte, Methoden, Experimente*; Wiley VCH: Weinheim, 1998; pp 414 – 418.
23. Wöhrle, D.; Gitzel, J.; Okura, I.; Aono, S. *J. Chem. Soc., Perkin Trans II* **1985**, 1171.
24. (a) Leest, R. E. V. D. *J. Electroanal. Chem.* **1973**, *43*, 251. (b) Sweetser, P. B. *Anal. Chem.* **1967**, *39*, 979.
25. Farrington, J. A.; Ebert, M.; Land, E. J. *J. Chem. Soc., Faraday Trans 1* **1978**, *74*, 665.
26. (a) Levey, G.; Rieger, A. L.; Edwards, J. O. *J. Org. Chem.* **1981**, *46*, 1255. (b) Levey, G.; Ebbesen, T. W. *J. Phys. Chem.* **1983**, *87*, 829.

27. (a) Dodge, A. D. *Endeavour* **1971**, *30*, 130. (b) Farrington, J. A.; Ebert, M.; Land, E. J.; Fletcher, K. *Biochim. Biophys. Acta* **1973**, *314*, 372. (c) Patterson, L. K.; Small, R. D.; Scaiano, J. C. *Radiat. Res.* **1977**, *72*, 218.
28. te Velde, G.; Bickelhaupt, F. M.; Baerends, E. J.; Guerra, C. F.; van Gisbergen, S. J. A.; Snijders, J. G.; Ziegler, T. *J. Comput. Chem.* **2001**, *22*, 931.
29. van Lenthe, E.; Snijders, J. G.; Baerends, E. J. *J. Chem. Phys.* **1999**, *105*, 6505.